Supplemental information for Korhonen, Lampinen et al.

Supplemental Methods

Leakage analysis. For the analysis of vascular leakage in the tracheal blood vessels, mice were injected with Ad-control or Ad-COMP-Ang1 (Ad-CAng1) two days prior to 16 h LPS challenge. Fluorescent 100 nm microspheres (Life Technologies) were injected via the tail vein and 4 min later, the mice were perfused with 10 ml of PBS or 10 ml of 1% PFA/PBS via the left ventricle, followed by collection of the tracheas for analysis.

TNF-α and soluble TNF-α receptor treatments. TNF-α (0.02 mg/kg, PeproTech) was injected via the tail vein and serum and tracheas were collected 30 min or 1 h later. Soluble TNF-α receptor (Etarnecept, 30 mg/kg, Wyeth) was injected intraperitoneally 1 hour prior to TNF-α or LPS injection. Control mice received PBS injection.

ELISA. ANG2 protein in serum was measured by ANG2 ELISA (R&D) and TNF-α by Magnetic Luminex Screening Assay (R&D).

Analysis of leukocyte counts in blood. Whole blood was collected by heart puncture in EDTA-capillaries (Hirschmann laborgerate). Leukocyte counts were measured using Exigo automated blood analyzer (Boule Medical AB).

β_1-integrin blocking assay. HUVECs were treated for 5 min with β_1-integrin blocking rat anti-human CD29 antibody (Clone Mab13, 500 μg/ml, BD Biosciences), or Armenian Hamster IgG (1 mg/ml, AbD Serotec, A Bio-Rad Company) as a control, and then with COMP-Ang1 (CAng1, 200 ng/ml) for 30 min. Tie2 was immunoprecipitated and analyzed using Western blotting.

Live imaging. Live imaging of HUVECs was performed using Zeiss LSM 880 confocal microscope inserted in an environmentally controlled incubator PM S1 (CO_2 5%, +37^{o}C), and with 63x Plan-Apochromat Oil-immersion objective NA 1.40 and Argon laser (488 nm). Z-stacks were recorded before stimulation and following angiopoietin stimulations (200 ng/ml) every 20 seconds. Videos were produced from maximum projections of the Z-stack images using LSM Zen software (Carl Zeiss). Alternatively, Zeiss Stallion live imaging system connected to Zeiss AxioCamMRm was used. GFP images were collected and saved as a stack file, which was converted to a video file.

IncuCyte apoptosis assay. For the simultaneous determination of apoptosis and proliferation in the IncuCyte® ZOOM system, HUVECs were cultured until they reached 80-90% confluence, treated with lentiviruses encoding shTie1 or shScrambled (shScr) for 1 day, and then cultured under puromycin (2 μg/ml) selection for 2 days. Cells were detached with trypsin, transferred into gelatin-coated 96-well plates (10.000 cells per a well) and allowed to attach. Immediately before the experiment, the medium was replaced with fresh full (FM) or serum-free (SF) medium and IncuCyte Caspase-3/7 reagent (Essen Bioscience, cat. # 4440) was added. The cells were analyzed in the Real-Time Quantitative Live-Cell imaging system IncuCyte® ZOOM at 1.5 h

intervals. Quantification of the apoptotic cells by green fluorescence signal was done with the IncuCyte ZOOM® Software (2015A).

***Tissue preparation, immunofluorescence staining, microscopy and analysis*.** For whole mount staining, the tracheas and ears were fixed in 1-4% PFA for 1 hour at RT, followed by several washes with PBS. The tissues were treated with Donkey immunomix blocking buffer (5% donkey serum, 0.2% BSA, 0.05% sodium azide and 0.3% Triton X-100 in PBS) for two hours and incubated in primary antibodies, diluted in the blocking buffer, at +4°C for 1-3 days or overnight at RT. For detection of the primary antibodies, the whole mounts were incubated with Alexa fluorochrome conjugated secondary antibodies (Life Technologies) for overnight at +4°C or RT. The samples were mounted with Vectashield mounting medium containing DAPI (Vector Labs, H-1200). To detect β-galactosidase activity in the *Tie1*$^{+/LacZ}$ mice the tracheas were processed as previously described (1).

Fluorescently labeled whole mount samples were imaged using a confocal microscope (Zeiss LSM 780, LSM 880, or LSM 510) in multichannel mode. Three-dimensional projections were digitally reconstructed from confocal z-stacks using the LSM software (Carl Zeiss). Average postcapillary venule and capillary diameter was measured from 5-6 vessels over 6-8 cartilage rings in each trachea (2) with Image J. P-selectin and EPHB4 areas were calculated with ImageJ and normalized to PECAM1 area in each microscopic field. The amount of proliferating endothelial cells was calculated as percentage of Ki67-positive endothelial cells per PECAM1-positive vessel area. Staining for Tie1 and Tie2 in tracheal blood vessels were analyzed by calculating the staining intensity per vessel. Number of Cd11b+ cells were counted manually per

microscopic field. Leakage was analyzed by calculating the percentage of microsphere area in each microscopic field. Fractional areas (area densities) of pTie2, FOXO1, vWF and Ang2 were normalized to PECAM1.

For immunofluorescence staining of HUVECs, the cells were fixed with 4% PFA for 10 min, permeabilized with 0.1% Triton-X in PBS for 5 min, blocked with 1% BSA-PBS (Biotop), stained using primary antibodies for 30 min at room temperature, washed, stained with secondary fluorescently conjugated antibodies (Life Technologies) when appropriate and for nuclei using Hoechst (Sigma-Aldrich) and mounted using Mowiol-Dabco (Sigma-Aldrich). For FRET/FLIM analysis, the cells were stained using mouse anti-V5-cy3 (clone V5-10, Sigma-Aldrich, V8012), and mounted with Vectashield medium (Vector Laboratories).

Preparation of protein lysates and western blotting. The lungs were lysed with 0.5% TX-100 and 0.5% NP-40 in PBS (for total lysates) or with RIPA buffer (for immunoprecipitation) (50 mM Tris-HCl pH 7.4, 1% NP-40, 0.25% Na-deoxycholate, 150 mM NaCl, 1 mM EDTA) containing protease inhibitors (1 mM PMSF, 1 mg/mL each aprotinin and leupeptin, 1 mM Na_3VO_4 and 1 mM NaF) using 1.4 mm Ceramic Bead Tubes (MO BIO Laboratories). Cells were lysed in a lysis buffer (150 mM NaCl, 5% glycerol, 1% Triton X-100, 1.5 mM $MgCl_2$, 1 mM EGTA, 10 mM $Na_4P_2O_7 \cdot 10\ H_2O$, 100 mM NaF, 50 mM Hepes, 1 mM Na_3VO_4, PMSF, aprotinin, and leupeptin). For detection of soluble serum proteins, 2.5 ul of serum per sample was mixed with lysis buffer. Protein concentration of the lysates was measured using the PierceBCA Protein Assay kit (Thermo Scientific). Equal amounts of total protein were used for immunoprecipitation with primary antibodies and the protein G–Sepharose (GE Healthsciences

Ab) or the protein G/A–Sepharose (Santa Cruz Biotechnology) at +4°C. The immunocomplexes or total lysates were separated in SDS-PAGE (Ready-Gels; Bio-Rad Laboratories), transferred to TransBlot Turbo Midi-size PVDF membrane (Bio-Rad Laboratories) using the Trans-Blot Turbo Transfer System (Bio-Rad Laboratories) or transferred to a nitrocellulose membrane (PerkinElmer). Membranes were used for immunoblotting with primary antibodies, HRP-conjugated secondary antibodies (Dako) or biotinylated secondary antibodies (Dako) and Streptavidin-Biotinylated-Horseradish Peroxidase conjugate (GE-Healthcare) followed by ECL detection with the SuperSignal West Pico Chemiluminescent Substrate or SuperSignal West Femto Maximun Sensitivity Substrate (Thermo Scientific). Western blots were captured on a film or imaged with Odyssey FC (LI-COR). For reprobing, the membranes were stripped using the RePlot Plus Strong Antibody stripping buffer (Millipore). Western blots were quantified using ImageJ.

RNA isolation and qRT-PCR analysis. Total RNA from lungs and tracheas was isolated using the NucleoSpin RNA II Kit (Macherey-Nagel). RNA was reverse-transcribed using the iScript cDNA Synthesis Kit (Bio-Rad) according to the manufacturer's instructions. qRT-PCR reactions were carried out using the iQ Supermix (Bio-Rad) or the iQ SYBR Green Supermix (Bio-Rad) and a BIO-RAD C1000 Thermal cycler according to standardized protocols. The TaqMan Gene Expression Assays used for mouse mRNA were: *Gapdh* (4352932E), *Pecam1/CD31* (M*m01246167_m1), Tie1* (*Mm00441786_m1*), *Esm1* (Mm00469953_m1), *Tie2/Tek* (Mm00443242_m1), *Angpt2/Ang2* (Mm00545822_m1), and *Angpt1/Ang1* (Mm00456503_m1). The SYBR Green probes were: *Tnf* (fwd. CCCTCACACTCAGATCATCTTCT, rev. GCTACGACGTGGGCTACAG) and *Il1b* (fwd. CTGGTGTGTGACGTTCCCATTA, rev.

CCGACAGCACGAGGCTTT). The data were normalized to *Pecam1* and *Gapdh*. Fold changes were calculated using the comparative CT (threshold cycle) method.

Antibodies. The following antibodies were used for immunofluorescence (IF), immunoprecipitation (IP) and western blotting (WB): goat anti-hTie2 (R&D Systems, AF313, IF, IP, WB), goat anti-hVEGF-R2/KDR (R&D Systems, AF357, IP, WB), mouse anti-hIntegrin β_1 (Merck Millipore, MAB2252), rabbit anti-hIntegrin β_3 (Abcam, Ab75872, WB), goat anti-hIntegrin-alpha$_5$/CD49e (R&D Systems, AF1864, WB), mouse anti-hIntegrin β_1 (12G10) (Abcam, ab30394), rabbit anti-hEEA1 (Cell Signaling, C45B10, IF), mouse anti-Hsc70 (Santa Cruz Biotechnology, sc-7298, WB), mouse anti-phospho-tyrosine (pTyr) (Merck Millipore, clone 4G10, 05-321, WB), rabbit anti-Tie1 (Santa Cruz Biotechnology, sc-342, WB), goat anti-hTie1 (R&D Systems, AF619, WB, IF), rabbit anti-Akt (Cell Signaling, 9272, WB), rabbit anti-p-Akt (Ser473) (Cell Signaling, 9271 or 4060, WB), rabbit anti-Flag (Sigma, F7425, WB), rabbit anti-β–actin (Cell Signaling, 4967, WB), goat anti-hAng2 (R&D Systems, AF623, WB), goat anti-m/rTie2 (R&D Systems, AF762, IP, WB, IF), mouse anti-pTyr (Santa Cruz, clone PY99, sc-7020, WB), rabbit anti-FOXO1 (Cell signaling, 2880, IF), hamster anti-mCD31 (PECAM1, Chemicon, AB-13982Z, IF), rat anti-mCD31 (PECAM1, BD Biosciences, 550274, IF), goat anti-mP-selectin (R&D Systems, AF737, IF), goat anti-mEphB4 (R&D Systems, AF446, IF), rabbit anti-Ki67 (Abcam, ab16667, IF), rat anti-CD11b (eBioscience, 14-0112-81, IF), rabbit anti-phospho-Tie2 (Y992, R&D, AF2720, IF), human anti-Ang2 (IF, kind gift from MedImmune) (3), human-anti-Tie2 (REGN1376, IF) (4), human anti-Ang2 (REGN910, IF) (5), rabbit anti-vWF (Dako, A0082, IF) and Alexa-488, Alexa-594, Alexa-647-conjugated secondary antibodies (Life Technologies).

***Expression vector cloning*.** Tie1 and Tie2 plasmids used for FLIM/FRET were constructed as follows. Tie2-GFP is hTie2 fusion protein containing the Tie2 amino acids 1-770 fused to eGFP in the C-terminus. The Tie2-GFP-pMXS was created by PCR from the FL-Tie2-eGFP-pMXS vector backbone (6) using SphI and SacII restriction enzymes. Tie1-V5-pMXS, coding for the hTie1 amino acid residues 1-838 and a C-terminal V5-tag, was created by PCR and inserted to the pMXS vector with SphI and NotI restriction enzymes. Full-length (FL) FL-Tie2-GFP-pMXS (6) and FL-Tie1-mCherry, containing eGFP and mCherry as C-terminal tags replacing the stop codons, respectively, were used for live imaging. The VE-cadherin-V5-pMXS vector was constructed by replacing the C-terminus of VE-cadherin in pMXS vector with an ApaI-NotI PCR fragment containing V5-tag (VE-cadherin plasmid was a kind kift from Dr. Elisabetta Dejana, University of Milan, Italy). The membrane-anchored eGFP has been previously described (7).

References

1. D'Amico, G., Korhonen, E.A., Anisimov, A., Zarkada, G., Holopainen, T., Hagerling, R., Kiefer, F., Eklund, L., Sormunen, R., Elamaa, H., et al. 2014. Tie1 deletion inhibits tumor growth and improves angiopoietin antagonist therapy. *J Clin Invest* 124:824-834.
2. Kim, K.E., Cho, C.H., Kim, H.Z., Baluk, P., McDonald, D.M., and Koh, G.Y. 2007. In vivo actions of angiopoietins on quiescent and remodeling blood and lymphatic vessels in mouse airways and skin. *Arterioscler Thromb Vasc Biol* 27:564-570.
3. Holopainen, T., Saharinen, P., D'Amico, G., Lampinen, A., Eklund, L., Sormunen, R., Anisimov, A., Zarkada, G., Lohela, M., Helotera, H., et al. 2012. Effects of angiopoietin-2-blocking antibody on endothelial cell-cell junctions and lung metastasis. *J Natl Cancer Inst* 104:461-475.
4. Adler, A., Daly, C., Parveen, A., Nevins, T., Shan, J., Fairhurst, J., Huang, T., Martin, J., Papadopoulos, N., Yancopoulos, G., et al. 2014. Blockade of angiopoietin-2 or Tie2 is equally effective at inhibiting tumor growth and reducing tumor vessel density in most human tumor xenograft models *Cancer Research* 74:4492.
5. Daly, C., Eichten, A., Castanaro, C., Pasnikowski, E., Adler, A., Lalani, A.S., Papadopoulos, N., Kyle, A.H., Minchinton, A.I., Yancopoulos, G.D., et al. 2013. Angiopoietin-2 functions as a Tie2 agonist in tumor models, where it limits the effects of VEGF inhibition. *Cancer Res* 73:108-118.

6. Saharinen, P., Eklund, L., Miettinen, J., Wirkkala, R., Anisimov, A., Winderlich, M., Nottebaum, A., Vestweber, D., Deutsch, U., Koh, G.Y., et al. 2008. Angiopoietins assemble distinct Tie2 signalling complexes in endothelial cell-cell and cell-matrix contacts. *Nat Cell Biol* 10:527-537.
7. Hakanpaa, L., Sipila, T., Leppanen, V.M., Gautam, P., Nurmi, H., Jacquemet, G., Eklund, L., Ivaska, J., Alitalo, K., and Saharinen, P. 2015. Endothelial destabilization by angiopoietin-2 via integrin beta1 activation. *Nat Commun* 6:5962.

Supplemental Video Legends

Supplemental Video 1. Colocalization of FL-Tie2-GFP and FL-Tie1-mCherry in endothelial cell-cell junctions and intracellular vesicles following CAng1 stimulation. HUVECs were transduced with retroviral vectors coding for FL-Tie1 and FL-Tie2 receptors tagged in their C-termini with mCherry and GFP fluorescent proteins, respectively, starved and stimulated with 200 ng/ml CAng1, which was added after the first frame. GFP, mCherry and phase contrast images were collected every 5 min using the Zeiss Stallion live imaging system connected to Zeiss AxioCamMRm, saved as a stack file and converted into a video file (10 frames/second). Elapsed time is indicated as h : min : s. Note the colocalization of Tie1 and Tie2 signals as yellow color in cell-cell junctions and in intracellular vesicles detaching from the junctions. The Tie1-mCherry fusion protein that accumulates intracellularly does not colocalize with Tie2.

Supplemental Video 2-3. Accumulation of Tie2-GFP in endothelial cell junctions after ANG2 stimulation is decreased in Tie1 silenced cells. HUVECs transduced with retroviral vectors encoding FL-Tie2-GFP were transfected with shScr (Video 2) or shTie1 lentivirus (Video 3), starved and stimulated with 200 ng/ml ANG2 (R&D), which was added at time point

zero. Z-stack images were collected every 20 s and saved as a stack file. Maximum projections were generated using the LSM Zen software (Carl Zeiss) and converted into a video file (10 frames/second). Elapsed time is indicated as h : min : s.

Supplemental Video 4-5. Tie2-GFP internalization from endothelial junctions to vesicular structures in Tie1 silenced ANG1 stimulated HUVECs. HUVECs expressing FL-Tie2-GFP were transfected with shScr (Video 4) or shTie1 lentivirus (Video 5), starved and stimulated with 200 ng/ml ANG1 (R&D), which was added at time point zero. Z-stack images were collected every 20 s and saved as a stack file. Maximum projections were generated using the LSM Zen software (Carl Zeiss), and converted to a video file (10 frames/second). Elapsed time is indicated as h : min : s.

Supplemental Figure Legends

Supplemental Figure 1. Analysis of Tie1-Tie2 and Tie2-VE-cadherin interactions using acceptor photobleaching and frequency domain FLIM. (A) Representative confocal images of HUVECs analyzed for FRET in 1C and 1E, after acceptor photobleaching of regions of interest (ROI, dashed rectangles), with average FRET efficiency % calculated from the ROIs. For control n(ROI)=5 and cells treated with CAng1 n(ROI)=14, ANG1 n(ROI)=15 and ANG2 n(ROI)=14. (B) HUVECs were transduced with retroviral vectors expressing V5- and GFP-tagged Tie1 and Tie2 constructs (as in A, n(ROI)=14) or with Tie1-V5 and a membrane-anchored GFP (nROI)=5, as a control. Change in Tie2-GFP intensity in cells stimulated with CAng1 was detected using FRET after acceptor photobleaching. Representative confocal images

before (pre) and after (post) photobleaching of the Cy3 acceptor in ROI (lined area) are shown. Average FRET efficiency % -/+ SD. (C) Representative FLIM (spatial distribution of lifetime value) and fluorescent confocal images of HUVECs transduced with Tie2-GFP and VE-cadherin-V5, stimulated with CAng1, ANG1 or ANG2. GFP lifetime is indicated by the color change from red to blue in the left column. Arrows point to cell-cell junctions, where the GFP-lifetime was measured. (D) Quantification of the GFP lifetimes (ns) of HUVECs in A. n(ROI)=32 for unstimulated control, n(ROI)=44 for CAng1, n(ROI)=35 for ANG1 and n(ROI)=37 for ANG2 stimulated cells. Welch's unequal variances t-test, followed by Bonferroni's post hoc test. Error bars: SD. Scale bars: 20 μm (A) and (C), 10 μm (B).

Supplemental Figure 2. Effect of β_1-integrin on Tie1-Tie2 interaction using FLIM based on time correlated single photon counting (TCSPC) and FRET based on acceptor photobleaching. (A) Confocal FLIM based on TCSPC was performed on regions of interest (ROI, arrow) of samples shown in Fig 2A. Fitting of the GFP lifetime decay curves are presented on the right for ROI. IRF, Instrument response function. (B) shScr or β_1-integrin (shβ_1) silenced HUVECs expressing Tie2-GFP and Tie1-V5 were stimulated with CAng1. Representative confocal microscopic images after acceptor photobleaching of Cy3 in regions of interest (ROI, dashed rectangles). (C) Quantification of the change in GFP fluorescence intensity after Cy3 photobleaching. n(ROI)=4 for unstimulated shScr control, n(ROI)=6 for unstimulated shβ_1 cells, n(ROI)=11 for CAng1-stimulated shScr, n(ROI)=12 for CAng1-stimulated shβ1cells. ** $P < 0.01$; *** $P < 0.001$, Welch's unequal variances t-test, followed by Bonferroni's post hoc test. Error bars: SD. Scale bars: 20 μm.

Supplemental Figure 3. Effect of β_1- and β_3-integrin silencing on Tie2 localization in ANG1-stimulated HUVECs. HUVECs were transfected with shScr, shβ_1- and shβ_3-integrin lentiviruses, starved, stimulated with CAng1, fixed and stained for Tie2 and VE-cadherin. Nuclear DAPI shown in blue. Arrows point to cell junctions. A representative experiment is shown (shβ_1 n=4, shβ_3 n=2). Scale bar: 20 μm.

Supplemental Figure 4. β_1-integrin silencing reduces ANG1-induced FOXO1 translocation in HUVECs. (A) FOXO1 (red), DAPI (blue) and β_1-integrin (white) staining of control shScr and shβ_1−integrin silenced HUVECs stimulated with ANG1. Arrows point to FOXO1 negative nuclei. Scale bar: 20 μm. Representative confocal images (n=3). (B) HUVECs were treated with CAng1 and two different concentrations of β_1-integrin blocking (mAb13) or control antibodies, as indicated. Tie2 was immunoprecipitated and analyzed using Western blotting with anti-phosphotyrosine and Tie2 antibodies.

Supplemental Figure 5. Tie1 deletion or angiopoietin overexpression do not alter blood leukocytes or tracheal CD11b+ cell counts. (A) White blood cell (WBC) and (B) monocyte counts in blood from control or *Tie1*$^{i\Delta EC}$ mice treated with Ad-control, Ad-CAng1 or Ad-Ang2 for two weeks. (C) Quantification of CD11b+ cells in the trachea. (D) PECAM1 (red) and CD11b (green) whole mount staining in trachea. Scale bar: 50 μm. Error bars: SEM. n = 4-6.

Supplemental Figure 6. Tie1 silencing increases apoptosis rate in HUVECs only in serum-free conditions. Apoptosis was analyzed in shScr or shTie1 lentiviral vector-transfected HUVECs in normal full medium (FM) or in serum-free (SF) medium, using the IncuCyte

Caspase-3/7 reagent and IncuCyte® ZOOM equipment. Cell proliferation was determined by area coverage. Error bars: SEM. n = 4. ** P < 0.01, *** P < 0.001, 1-way ANOVA followed by Tukey's post hoc test.

Supplemental Figure 7. Tie1 deficiency reduces FOXO1 translocation after CAng1 treatment. Tracheal whole mount samples from control and Tie1 deleted mice treated with Ad-control or Ad-CAng1 for two days were stained for FOXO1 (red), PECAM1 (green) and DNA (DAPI, blue). Asterisks point to FOXO1-negative nuclei and hashes to FOXO1-positive nuclei. n = 4. Scale bar: 10 μm.

Supplemental Figure 8. ANG2 staining in tracheal blood vessels in ANG2 overexpressing mice. Tracheal whole mount samples from 10-12 month old control and $Ang2^{EC}$ mice in which ANG2 overexpression was induced since birth were stained for ANG2 (red) and PECAM1 (green). n = 2. Scale bar: 50 μm.

Supplemental Figure 9. Prolonged ANG2 expression increases blood leukocytes and tracheal CD11b+ cells. (A) Circulating white blood cell (WBC) and (B) monocyte counts in control mice and in transgenic mice induced to express ANG2 for 2-3 months after birth ($Ang2^{EC}$). (C) Quantification of CD11b+ cells in the tracheal whole mounts. (D) PECAM1 (green) and CD11b (red) staining of tracheas. Scale bar: 50 μm. Error bars: SEM. n = 7. * P < 0.05 vs. control, Student's t-test.

Supplemental Figure 10. Angiogenic effects of prolonged ANG2 expression in the trachea and skin. (A) ANG2 overexpression was induced since birth and tracheal blood vessels were visualized by PECAM1 staining in 11 month old control and *Ang2*^{EC} mice (in FVB background). (B) Ear skin blood vasculature was visualized by PECAM1 (green) or SMA (white) staining in 7 month old control and *Ang2*^{EC} mice. Arrows (*Ang2*^{EC}) and arrowheads (control) point to veins, asterisk marks a torturous artery and barb points to an arterial aneurysm. Note sites of arterial tortuosity (barb) and blood vessel dilation (arrows) in the *Ang2*^{EC} trachea and ear. Representative images (n = 3). Scale bars: 50 μm.

Supplemental Figure 11. Effect of Tie1 silencing on Tie2 phosphorylation and Tie2 trafficking in endothelial cells. (A) Representative confocal images of shTie1 and shScr lentivirus transfected FL-Tie2-GFP expressing HUVECs, stimulated with ANG2 and stained for phospho-Tie2. Nuclear DAPI stain is shown in blue. Scale bar: 20 μm. (B-C) Time point images of Supplemental Videos 2-5. HUVECs expressing FL-Tie2-GFP via retrovirus were silenced using shScr or shTie1 lentiviruses, starved and stimulated with ANG2 (B) or ANG1 (C). Scale bars: 20 μm. Angiopoietins were applied 20 s before the time point 0 min.

Supplemental Figure 12. Tie2 localization in EEA1 positive endosomes after ANG1 stimulation, and reduction of Tie2 protein in Ad-CAng1 treated Tie1 deficient mice. (A) FL-Tie2-GFP expressing HUVECs were stimulated for 10 minutes with ANG1 or ANG2, fixed and stained for EEA1. Representative images of maximum projections of confocal z-stacks are shown (n=2). Scale bar: 20 μm. Lines indicate the position of the Z-plane, which is shown on top and right sides of the images (not in scale). B) Quantification of Tie2 levels relative to β-actin

from lung lysates of control and *Tie1*$^{i\Delta EC}$ mice treated with Ad-control or Ad-CAng1 for two days. Error bars: SEM. n = 4. (*Pdgfb-iCreER*^{T2} deletor). * $P < 0.05$, 1-way ANOVA followed by Fisher's LSD post hoc test.

Supplemental Figure 13. Kinetics of LPS-induced Tie1 cleavage and downregulation of *Tie* and *Ang1* mRNAs. (A) Representative Tie1, Tie2, VCAM1 and β-actin western blotting of lung lysates of PBS or LPS treated mice at the indicated time points. Antibodies recognizing either Tie1 extracellular domain (ECD) or C-terminal tail (CT) were used. (B) qRT-PCR analysis of *Tie1* and *Tie2* mRNA fold changes in lungs at the indicated time points after LPS treatment, normalized to *Pecam1*. (C) qRT-PCR analysis of *Ang1* mRNA fold changes in lungs, normalized to *Gapdh*. n = 3-6 (except n = 2 for 12 h). ** $P < 0.01$, *** $P < 0.001$ vs. PBS control, 1-way ANOVA followed by Dunnett's post hoc test.

Supplemental Figure 14. TNF-α induces Tie1 cleavage in vivo. (A) qRT-PCR analysis of *Tnf* and *Il1b* mRNA fold changes in the lungs of PBS or LPS treated mice at the indicated time points, normalized to *Gapdh* mRNA expression. (B) TNF-α protein (ng/ml) in serum of LPS treated mice at the indicated time points. Error bars: SEM. ** $P < 0.05$, LPS 1 h (n = 3) vs. PBS control (n = 2), 1-way ANOVA followed by Dunnett's post hoc test. (C) Tie1 ECD (red) and PECAM1 (green) staining in tracheal blood vessels. Representative fluorescent images (n = 3). Scale bar: 10 μm. (D) Tie1 western blotting from serum of TNF-α, LPS and soluble TNF-α receptor (TNF-α inhibitor) treated mice at the indicated time points. Representative western blot (n = 3). (E) Tie1 western blotting from serum of TNFα, and TNFα +TNFα inhibitor treated mice at one hour after TNFα treatment. n = 2 (except for PBS control n = 1).

Supplemental Figure 15. Effect of LPS on Tie2 phosphorylation and FOXO1 expression. (A) Phospho-Tie2 (green), Tie2 (red) and PECAM1 (blue) staining in tracheal blood vessels of PBS or LPS treated mice. (B) Quantification of phospho-Tie2 relative to PECAM1 (%) at the indicated time points. (C) FOXO1 (green) and PECAM1 (red) staining. (D) Quantification of FOXO1 relative to PECAM1 (%). Scale bars: 20 μm. n = 3. * $P < 0.05$, ** $P < 0.01$, *** $P < 0.001$ vs. PBS control, 1-way ANOVA followed by Bonferroni's post hoc test.

Supplemental Figure 16. Effect of LPS on ANG2 expression and release. (A) vWF (green), ANG2 (red) and PECAM1 (blue) staining in tracheal blood vessels in PBS and LPS treated mice. Scale bar: 20 μm. (B) Quantification of vWF relative to PECAM1 (%) at the indicated time points. (C) Quantification of ANG2 relative to PECAM1 (%). n = 3. ** $P < 0.01$, *** $P < 0.001$ vs. PBS control, 1-way ANOVA followed by Bonferroni's post hoc test. (D) qRT-PCR analysis of *Ang2* mRNA fold changes in the lungs of PBS or LPS treated mice at the indicated time points, normalized to *Pecam1*. n = 3-6 (except n = 2 for 12 h). (E) Concentration of ANG2 protein in serum (ng/ml). n = 3-9 (except n = 2 for 0.5 and 12 h). ** $P < 0.01$, *** $P < 0.001$ vs. PBS control, 1-way ANOVA followed by Dunnett's post hoc test.

Supplemental Figure 17. ANG1 reduces LPS-induced leakage and ANG2 mRNA and protein. (A) Representative images of fluorescent microsphere leakage 16 h after LPS injection in tracheal blood vessels stained for PECAM1 (blue) in mice treated with Ad-control or Ad-CAng1. Vascular leakage was analyzed as explained in the Methods. Scale bar: 50 μm. (B) Quantification of microsphere area per field (%). (C) *Ang2* mRNA fold change in the lungs normalized to *Pecam1* and (D) ANG2 protein concentrations in serum 16 h after LPS injection.

n=3-10. Error bars: SEM. Scale bar: 50 μm. * $P < 0.05$, ** $P < 0.01$, *** $P < 0.001$, 1-way ANOVA followed by Tukey's post hoc test (B-C) or Student's t-test (D).

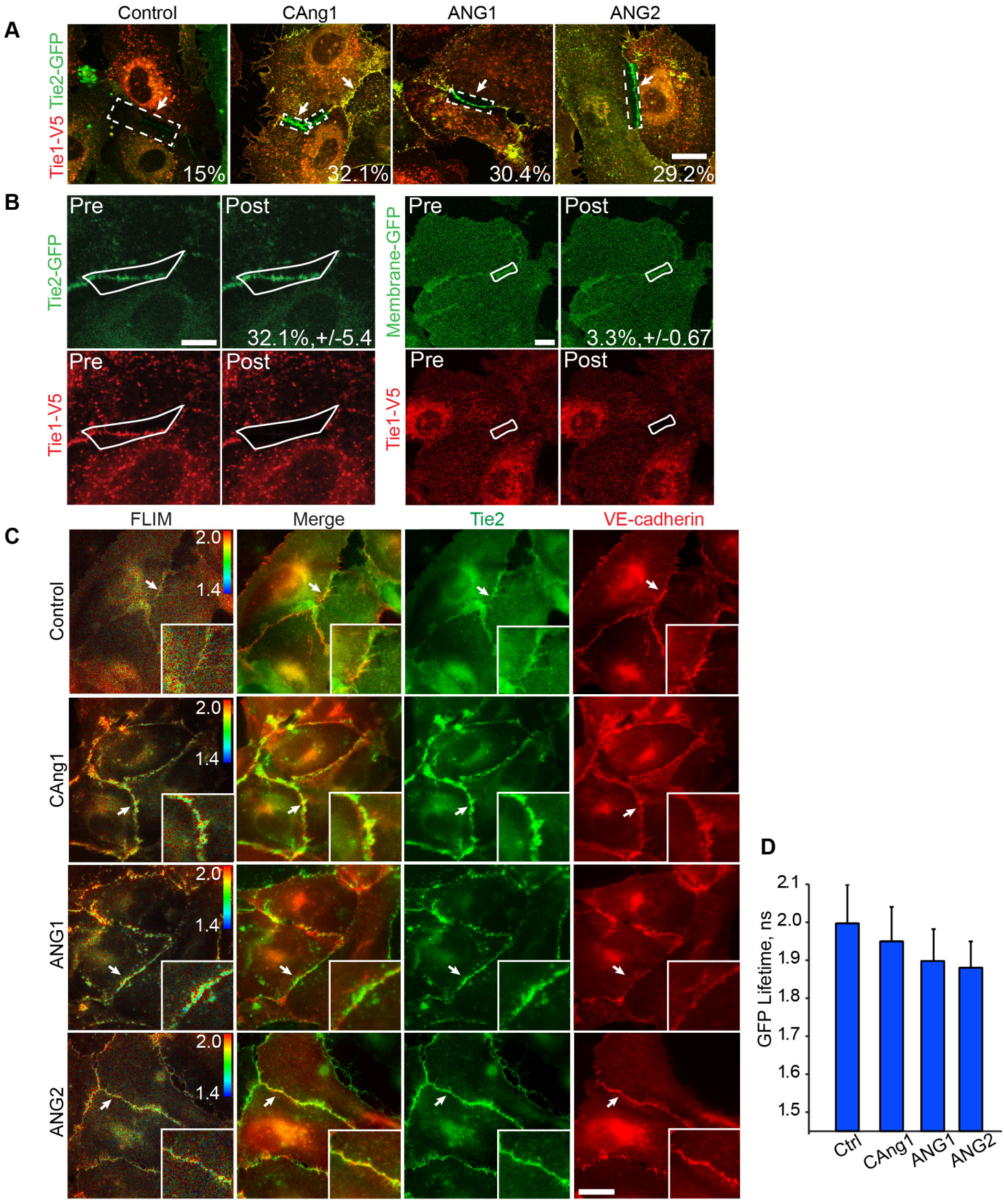

Supplemental Figure 1. Analysis of Tie1-Tie2 and Tie2-VE-cadherin interactions using acceptor photobleaching and frequency domain FLIM. (A) Representative confocal images of HUVECs analyzed for FRET in 1C and 1E, after acceptor photobleaching of regions of interest (ROI, dashed rectangles), with average FRET efficiency % calculated from the ROIs. For control n(ROI)=5 and cells treated with CAng1 n(ROI)=14, ANG1 n(ROI)=15 and ANG2 n(ROI)=14. (B) HUVECs were transduced with retroviral vectors expressing V5- and GFP-tagged Tie1 and Tie2 constructs (as in A, n(ROI)=14) or with Tie1-V5 and a membrane-anchored GFP (nROI)=5, as a control. Change in Tie2-GFP intensity in cells stimulated with CAng1 was detected using FRET after acceptor photobleaching. Representative confocal images before (pre) and after (post) photobleaching of the Cy3 acceptor in ROI (lined area) are shown. Average FRET efficiency % -/+ SD. (C) Representative FLIM (spatial distribution of lifetime value) and fluorescent confocal images of HUVECs transduced with Tie2-GFP and VE-cadherin-V5, stimulated with CAng1, ANG1 or ANG2. Decreased GFP lifetime is indicated by the color change from red to blue in the left column. Arrows point to cell-cell junctions, where the GFP-lifetime was measured. (D) Quantification of the GFP lifetimes (ns) of HUVECs in A. n(ROI)=32 for unstimulated control, n(ROI)=44 for CAng1, n(ROI)=35 for ANG1 and n(ROI)=37 for ANG2 stimulated cells. Welch's unequal variances t-test, followed by Bonferroni's post hoc test. Error bars: SD. Scale bars: 20 μm (A) and (C), 10 μm (B).

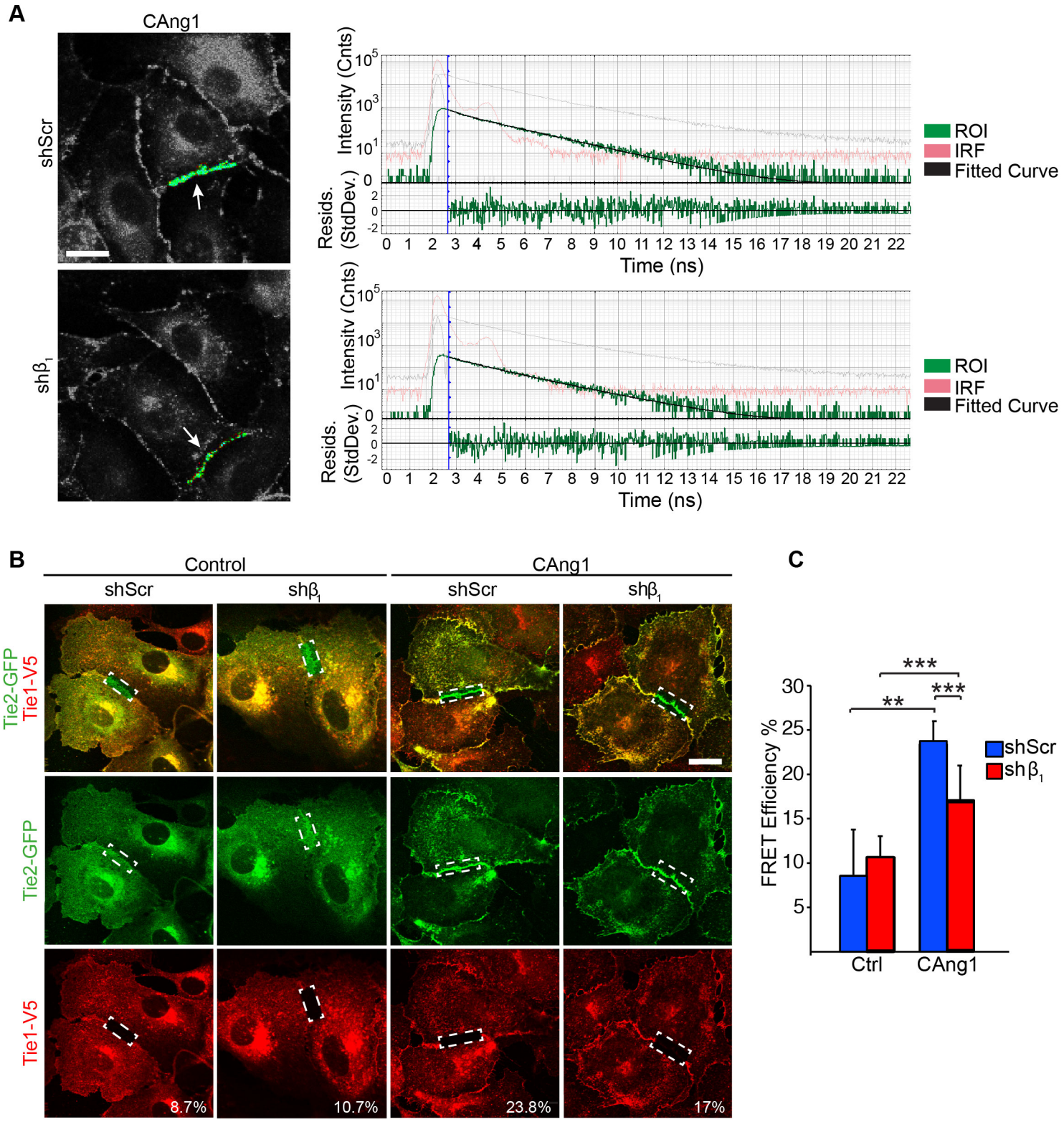

Supplemental Figure 2. Effect of β_1-integrin on Tie1-Tie2 interaction using FLIM based on time correlated single photon counting (TCSPC) and FRET based on acceptor photobleaching. (A) Confocal FLIM based on TCSPC was performed on regions of interest (ROI, arrow) of samples shown in Fig 2A. Fitting of the GFP lifetime decay curves are presented on the right for ROI. IRF, Instrument response function. (B) shScr or β_1-integrin (shβ_1) silenced HUVECs expressing Tie2-GFP and Tie1-V5 were stimulated with CAng1. Representative confocal microscopic images after acceptor photobleaching of Cy3 in regions of interest (ROI, dashed rectangles). (C) Quantification of the change in GFP fluorescence intensity after Cy3 photobleaching. n(ROI)=4 for unstimulated shScr control, n(ROI)=6 for unstimulated shβ_1 cells, n(ROI)=11 for CAng1-stimulated shScr, n(ROI)=12 for CAng1-stimulated sh$\beta_1$cells. ** $P < 0.01$; *** $P < 0.001$, Welch's unequal variances t-test, followed by Bonferroni's post hoc test. Error bars: SD. Scale bars: 20 µm (A) and (B).

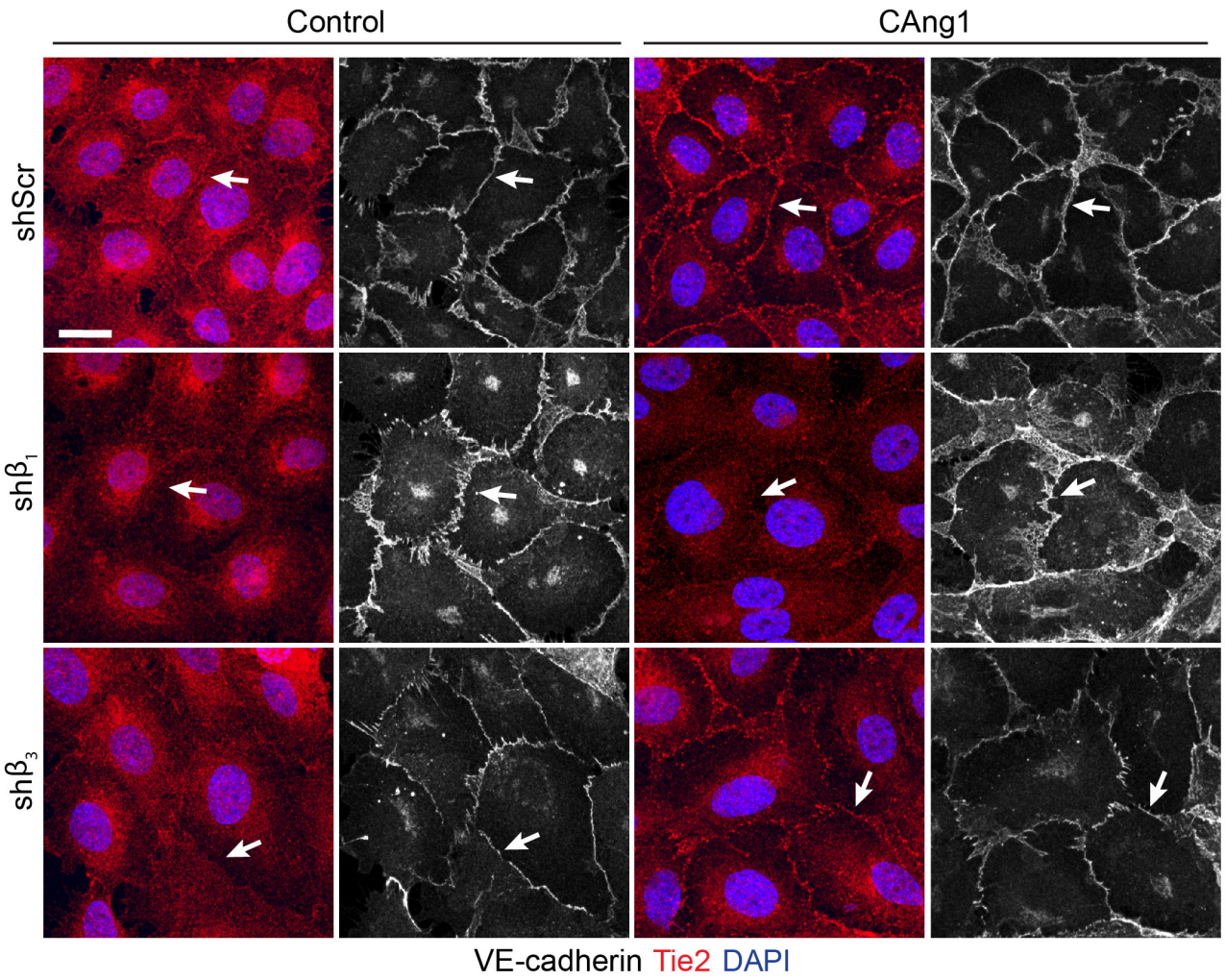

Supplemental Figure 3. Effect of β_1- and β_3-integrin silencing on Tie2 localization in ANG1-stimulated HUVECs. HUVECs were transfected with shScr, shβ_1- and shβ_3-integrin lentiviruses, starved, stimulated with CAng1, fixed and stained for Tie2 and VE-cadherin. Nuclear DAPI stain is shown in blue. Arrows point to cell junctions. A representative experiment is shown (shβ_1 n=4, shβ_3 n=2). Scale bar: 20 μm.

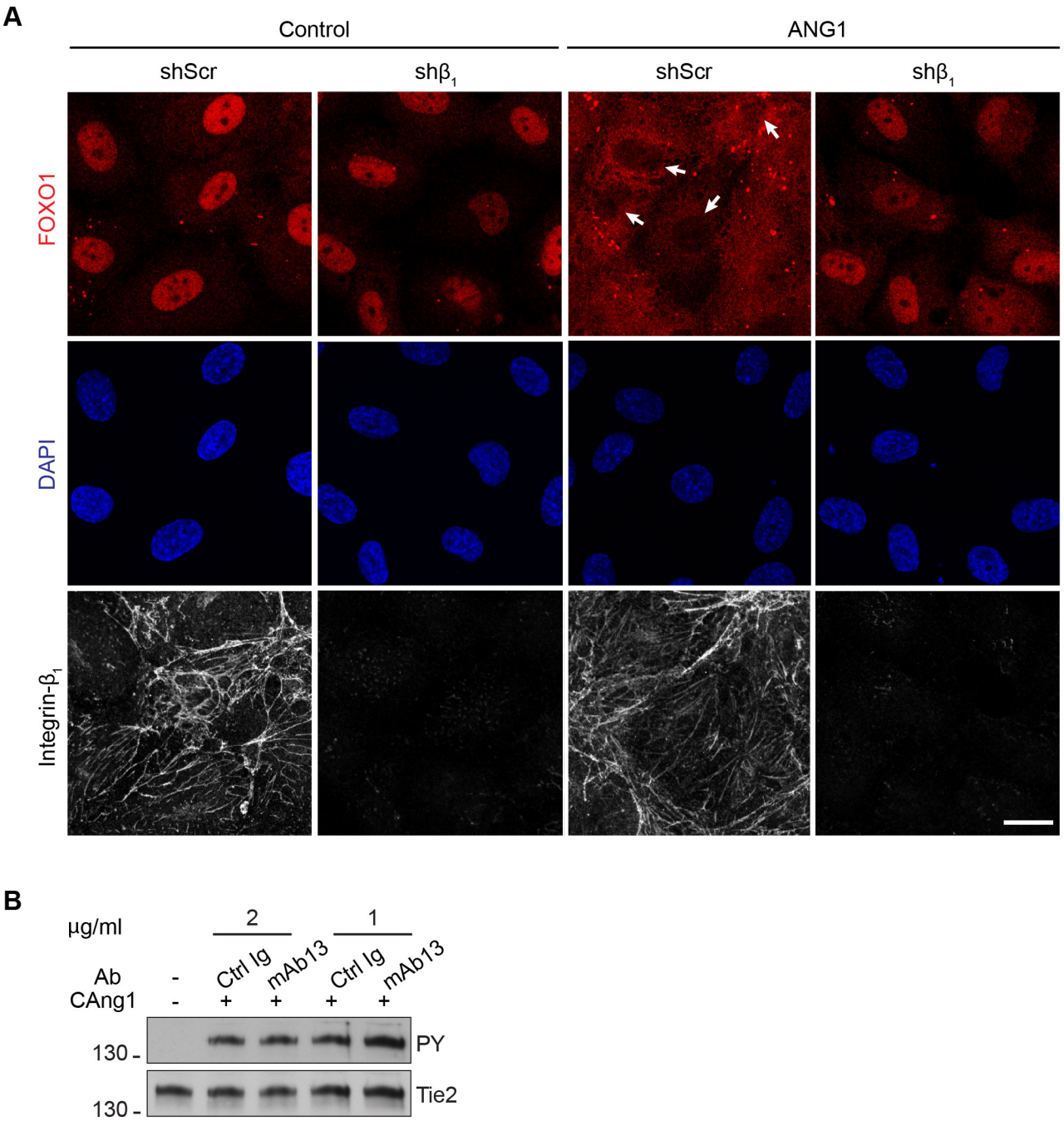

Supplemental Figure 4. β_1-integrin silencing reduces ANG1-induced FOXO1 translocation in HUVECs.
(A) FOXO1 (red), DAPI (blue) and β_1-integrin (white) staining of control shScr and shβ_1−integrin silenced HUVECs stimulated with ANG1. Arrows point to FOXO1 negative nuclei. Scale bar: 20 μm. Representative confocal images (n=3). (B) HUVECs were treated with CAng1 and two different concentrations of β_1-integrin blocking (mAb13) or control antibodies, as indicated. Tie2 was immunoprecipitated and analyzed using Western blotting with anti-phosphotyrosine and Tie2 antibodies.

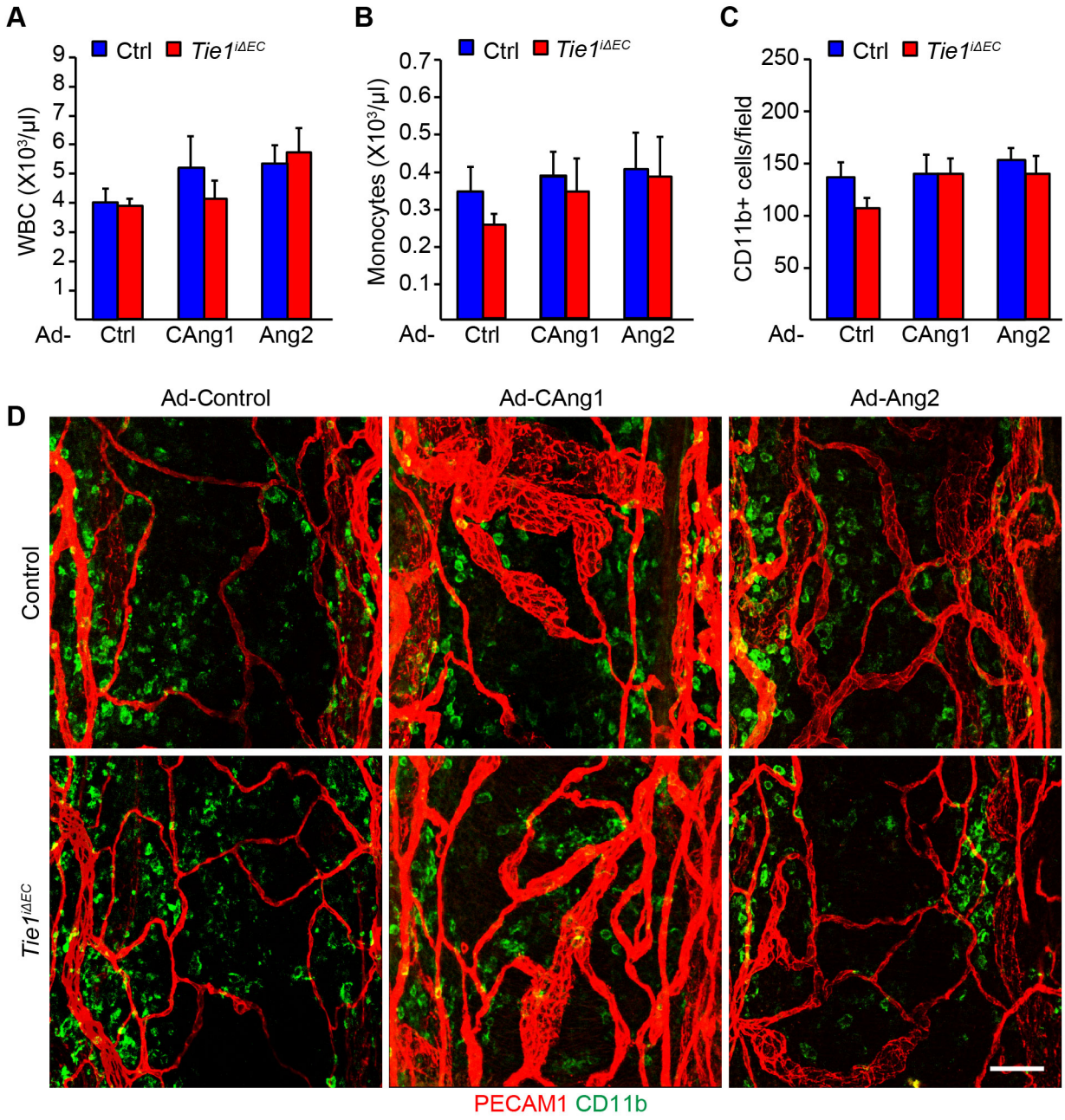

Supplemental Figure 5. Tie1 deletion or angiopoietin overexpression do not alter blood leukocytes or tracheal CD11b+ cell counts. (A) White blood cell (WBC) and (B) monocyte counts in blood from control or *Tie1*$^{i\Delta EC}$ mice treated with Ad-control, Ad-CAng1 or Ad-Ang2 for two weeks. (C) Quantification of CD11b+ cells in the trachea. (D) PECAM1 (red) and CD11b (green) whole mount staining in trachea. Scale bar: 50 μm. Error bars: SEM. n = 4-6.

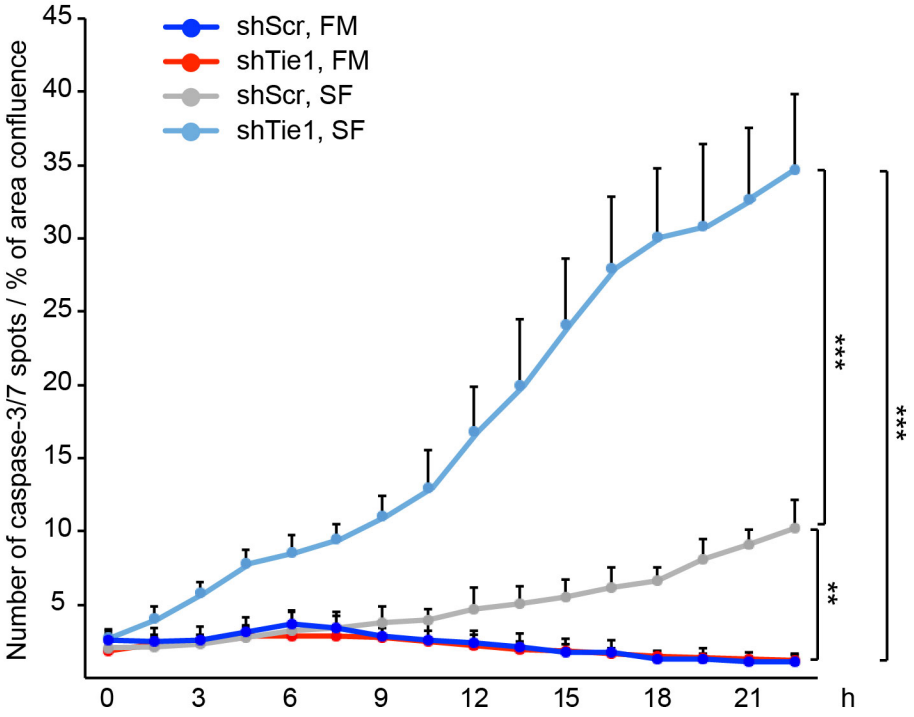

Supplemental Figure 6. Tie1 silencing increases apoptosis rate in HUVECs only in serum-free conditions. Apoptosis was analyzed in shScr or shTie1 lentiviral vector-transfected HUVECs in normal full medium (FM) or in serum-free (SF) medium, using the IncuCyte Caspase-3/7 reagent and IncuCyte® ZOOM equipment. Cell proliferation was determined by area coverage. Error bars: SEM. n = 4. ** P < 0.01, *** P < 0.001, 1-way ANOVA followed by Tukey's post hoc test.

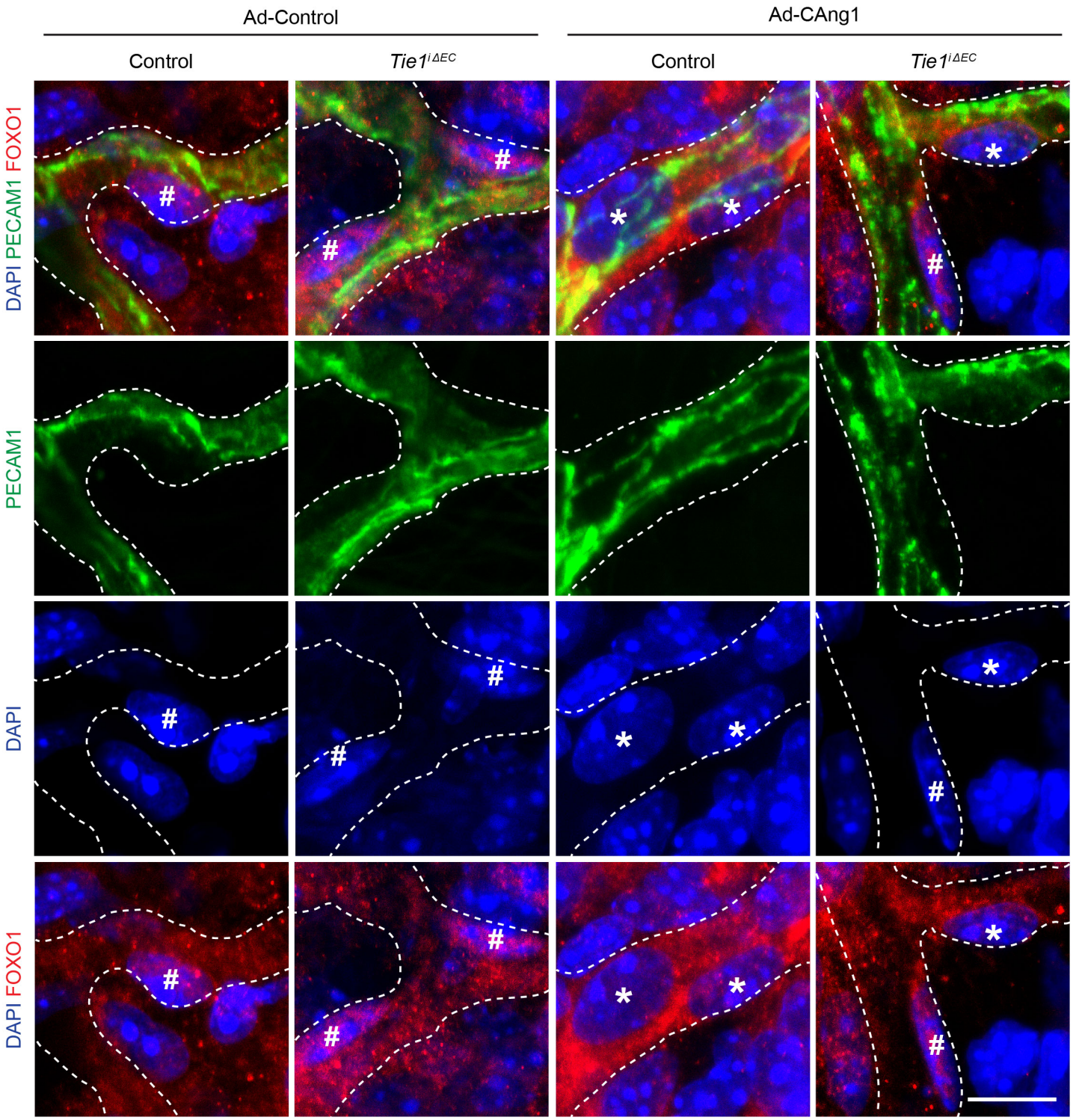

Supplemental Figure 7. Tie1 deficiency reduces FOXO1 translocation after CAng1 treatment. Tracheal whole mount samples from control and Tie1 deleted mice treated with Ad-control or Ad-CAng1 for two days were stained for FOXO1 (red), PECAM1 (green) and DNA (DAPI, blue). Asterisks point to FOXO1-negative nuclei and hashes to FOXO1-positive nuclei. n = 4. Scale bar: 10 µm.

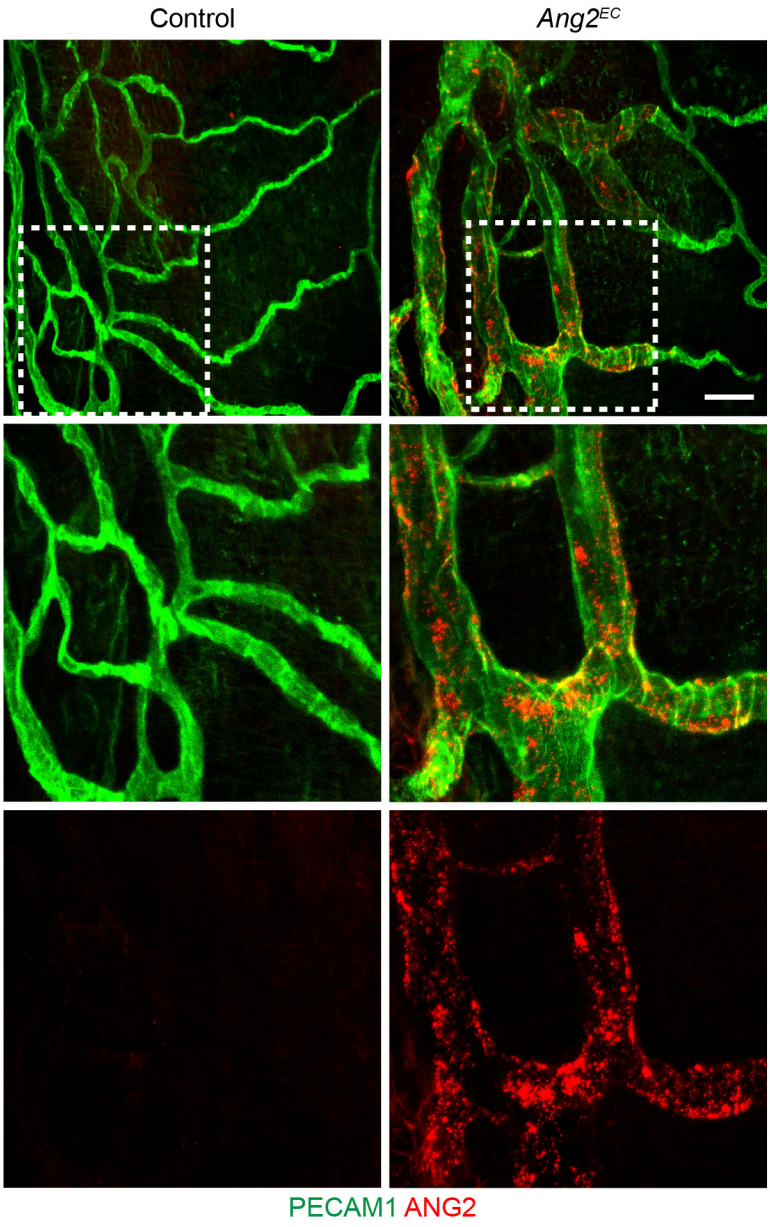

Supplemental Figure 8. ANG2 staining in tracheal blood vessels in ANG2 overexpressing mice. Tracheal whole mount samples from 10-12 month old control and *Ang2*^{EC} mice in which ANG2 overexpression was induced at birth were stained for ANG2 (red) and PECAM1 (green). n = 2. Scale bar: 50 µm.

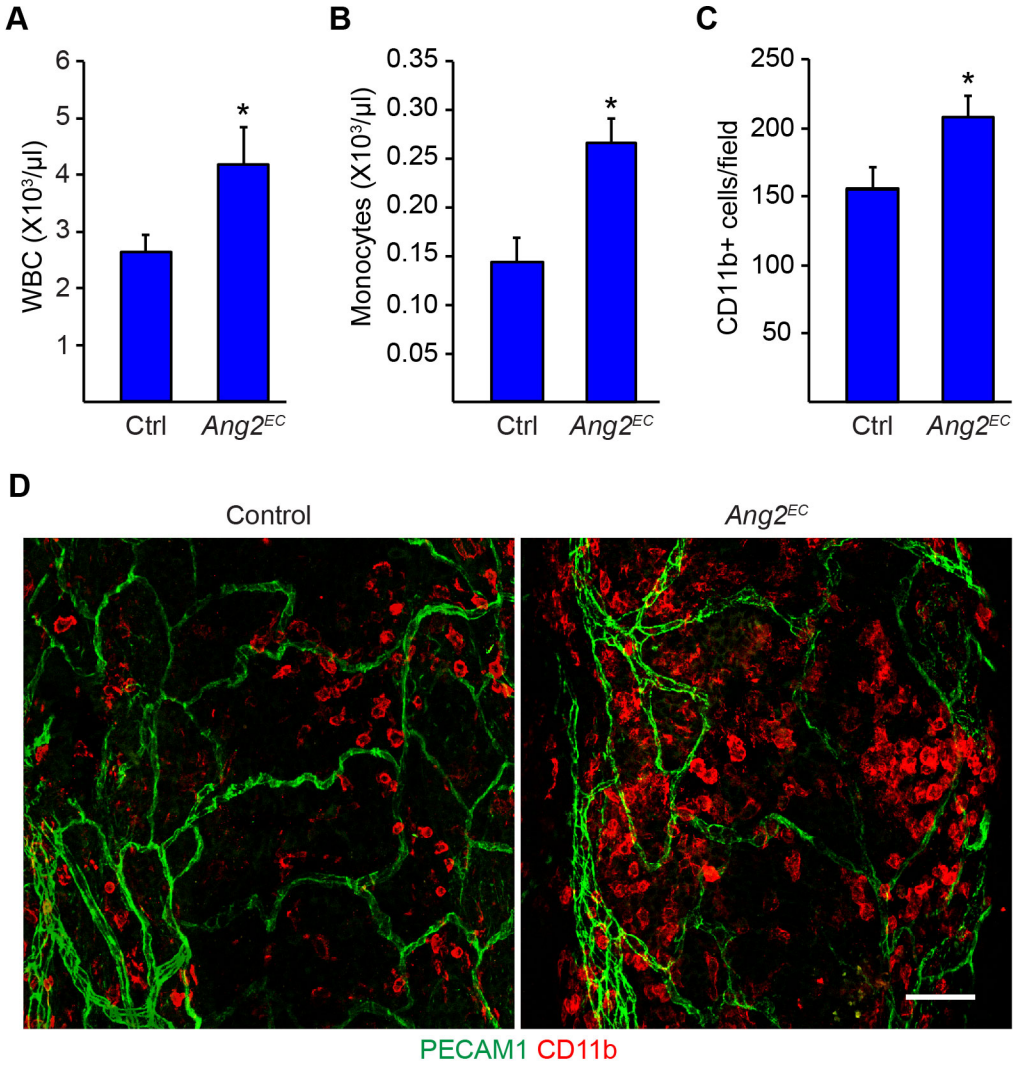

Supplemental Figure 9. Prolonged ANG2 expression increases blood leukocytes and tracheal CD11b+ cells. (A) Circulating white blood cell (WBC) and (B) monocyte counts in control mice and in transgenic mice induced to express ANG2 for 2-3 months after birth (*Ang2*^{EC}). (C) Quantification of CD11b+ cells in the tracheal whole mounts. (D) PECAM1 (green) and CD11b (red) staining of tracheas. Scale bar: 50 µm. Error bars: SEM. n = 7. * P < 0.05 vs. control, Student's t-test.

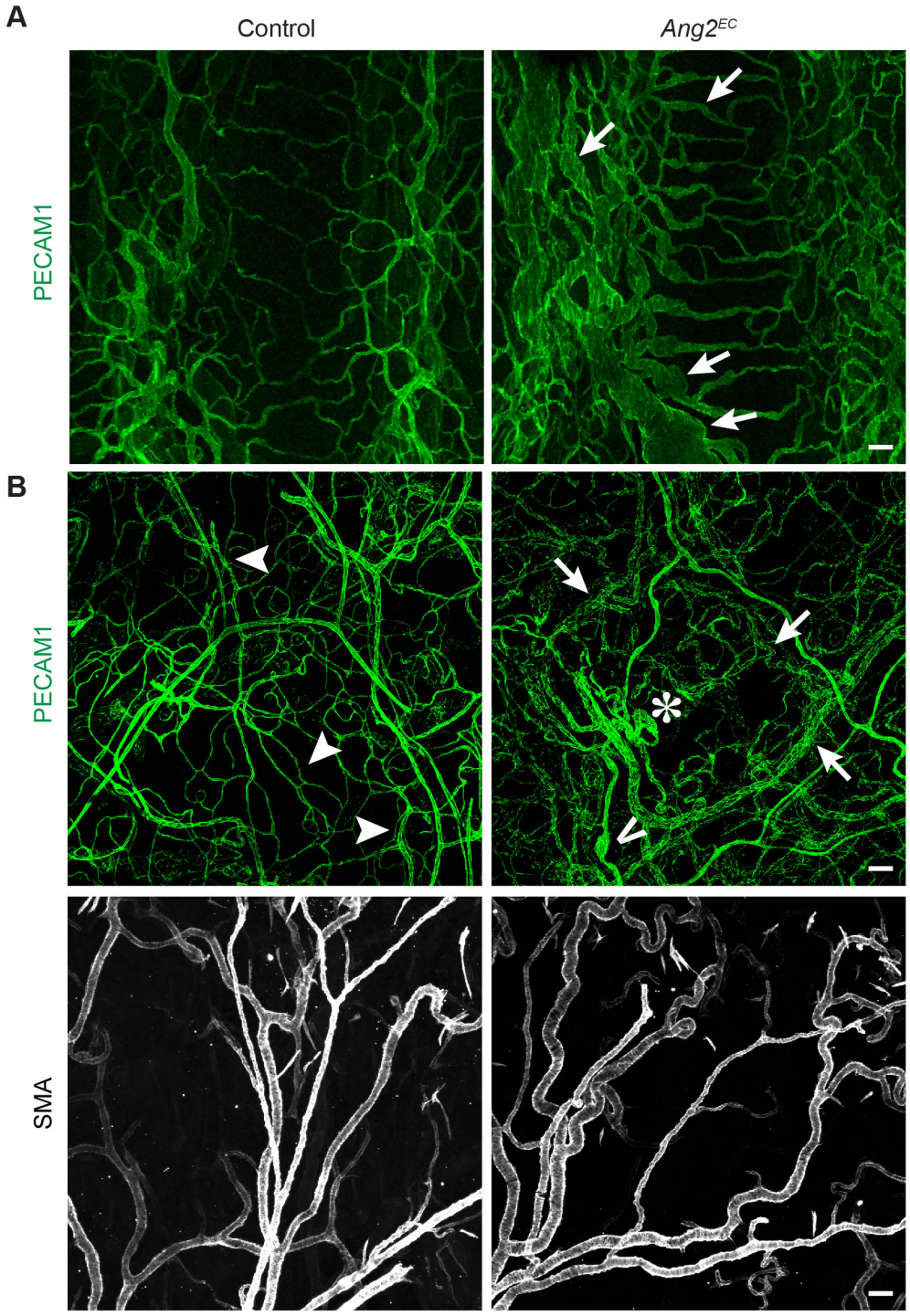

Supplemental Figure 10. Angiogenic effects of prolonged ANG2 expression in the trachea and skin. (A) ANG2 overexpression was induced since birth and tracheal blood vessels were visualized by PECAM1 staining in 11 month old control and *Ang2*^{EC} mice (in FVB background). (B) Ear skin blood vasculature was visualized by PECAM1 (green) or SMA (white) staining in 7 month old control and *Ang2*^{EC} mice. Arrows (*Ang2*^{EC}) and arrowheads (control) point to veins, asterisk marks a torturous artery and barb points to an arterial aneurysm. Note sites of arterial tortuosity (barb) and blood vessel dilation (arrows) in the *Ang2*^{EC} trachea and ear. Representative images (n = 3). Scale bars: 50 μm.

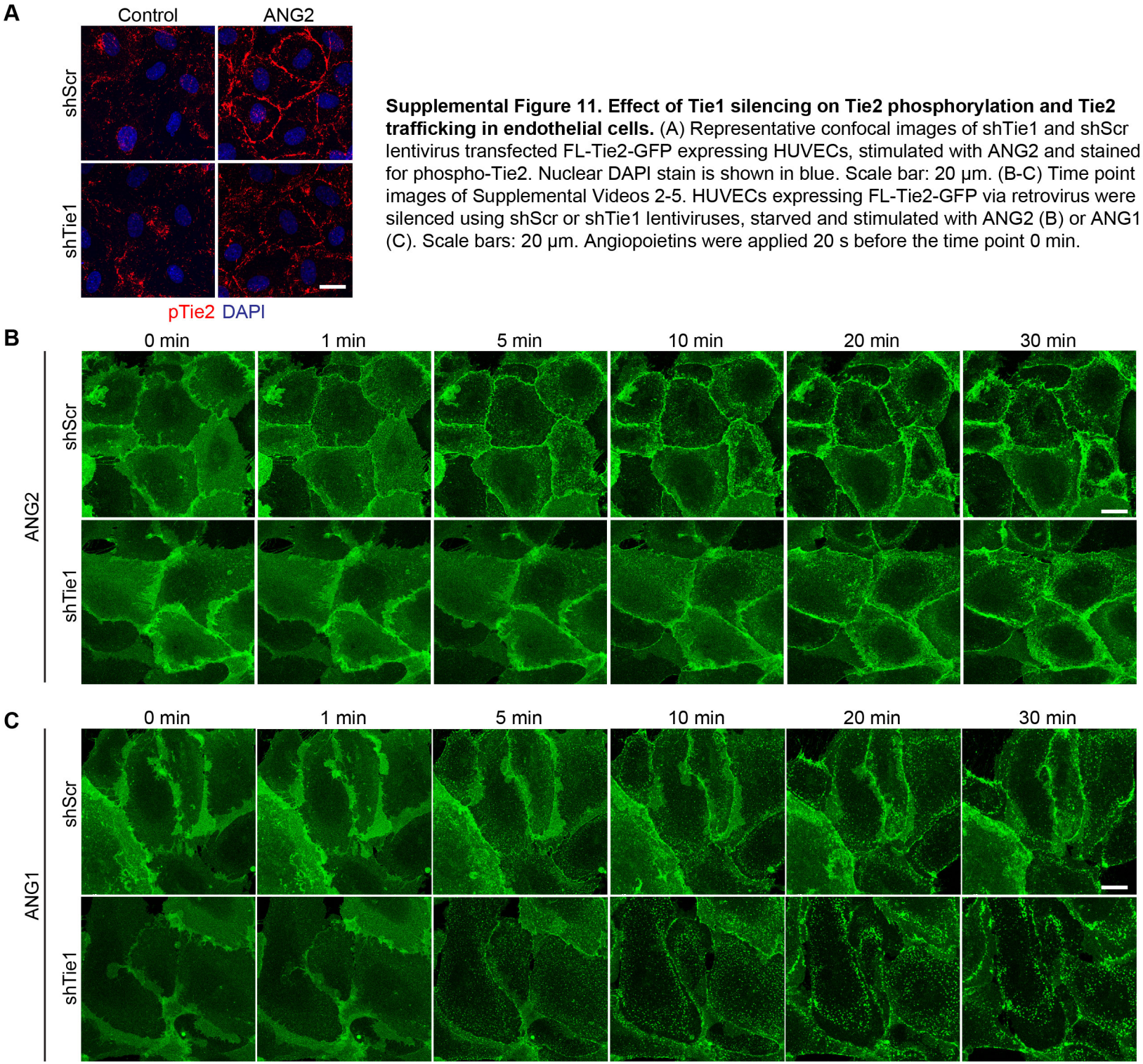

Supplemental Figure 11. Effect of Tie1 silencing on Tie2 phosphorylation and Tie2 trafficking in endothelial cells. (A) Representative confocal images of shTie1 and shScr lentivirus transfected FL-Tie2-GFP expressing HUVECs, stimulated with ANG2 and stained for phospho-Tie2. Nuclear DAPI stain is shown in blue. Scale bar: 20 μm. (B-C) Time point images of Supplemental Videos 2-5. HUVECs expressing FL-Tie2-GFP via retrovirus were silenced using shScr or shTie1 lentiviruses, starved and stimulated with ANG2 (B) or ANG1 (C). Scale bars: 20 μm. Angiopoietins were applied 20 s before the time point 0 min.

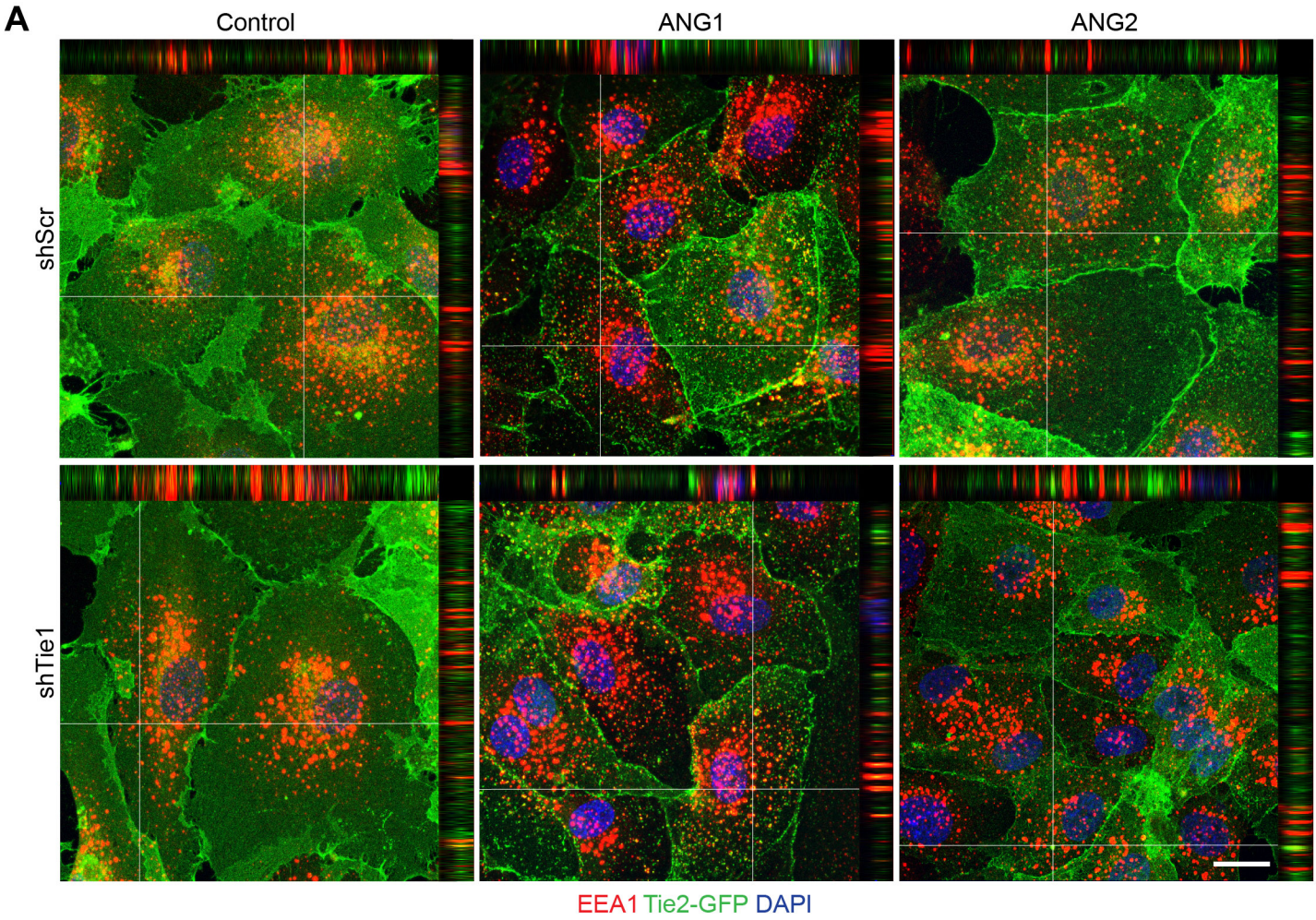

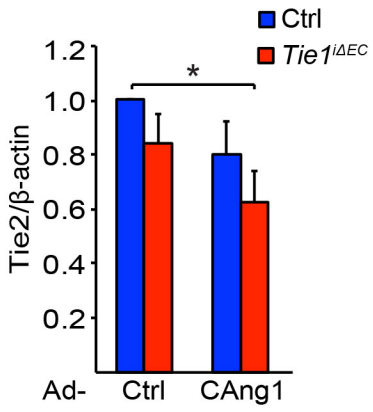

Supplemental Figure 12. Tie2 localization in EEA1 positive endosomes after ANG1 stimulation, and reduction of Tie2 protein in Ad-CAng1 treated Tie1 deficient mice. (A) FL-Tie2-GFP expressing HUVECs were stimulated for 10 minutes with ANG1 or ANG2, fixed and stained for EEA1. Representative images of maximum projections of confocal z-stacks are shown (n=2). Scale bar: 20 µm. Lines indicate the position of the Z-plane, which is shown on top and right sides of the images (not in scale). B) Quantification of Tie2 levels relative to β-actin from lung lysates of control and *Tie1*^{iΔEC} mice treated with Ad-control or Ad-CAng1 for two days. Error bars: SEM. n = 4. (*Pdgfb-iCreER*^{T2} deletor). * P < 0.05, 1-way ANOVA followed by Fisher's LSD post hoc test.

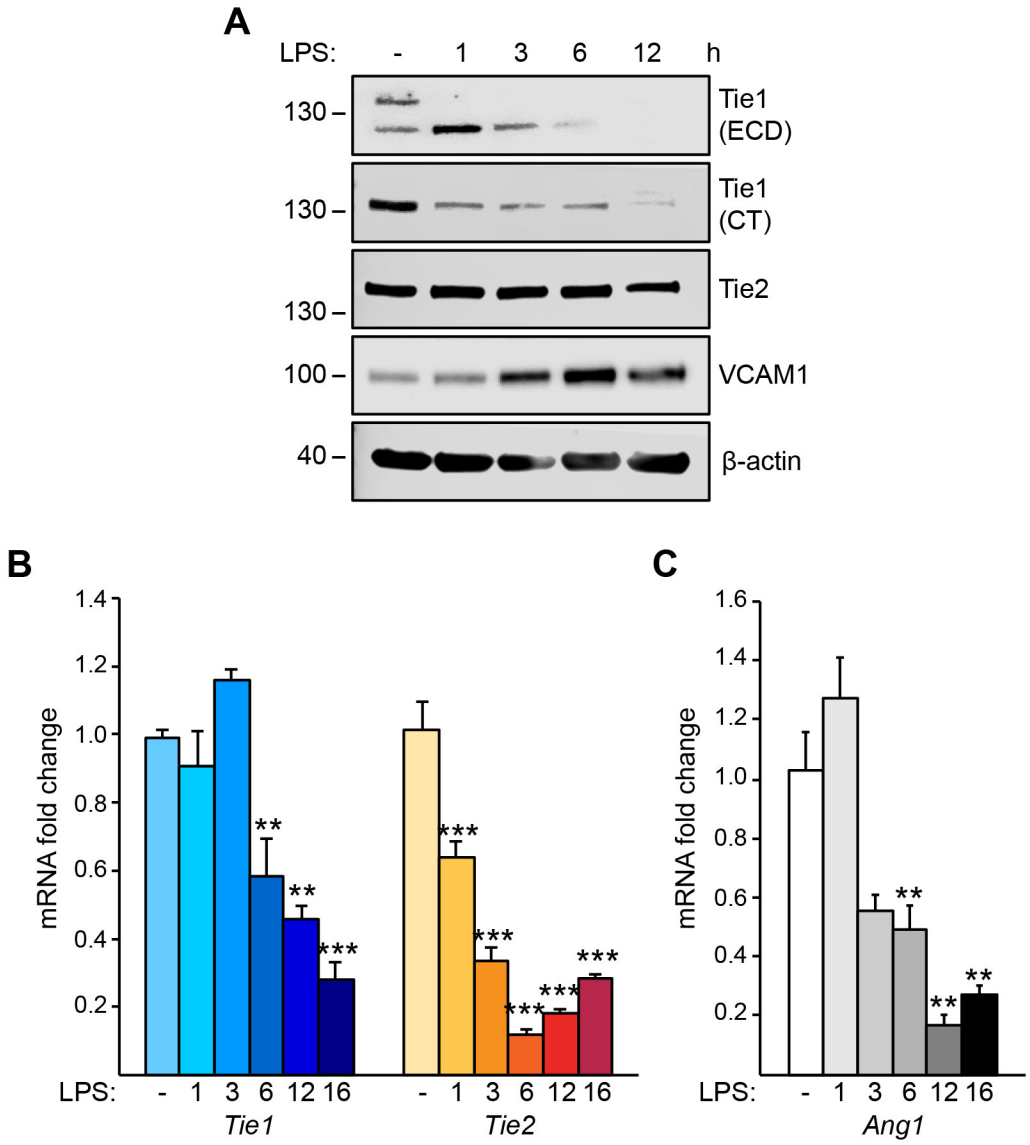

Supplemental Figure 13. Kinetics of LPS-induced Tie1 cleavage and downregulation of Tie and Ang1 mRNAs. (A) Representative Tie1, Tie2, VCAM1 and β-actin western blotting of lung lysates of PBS or LPS treated mice at the indicated time points. Antibodies recognizing either Tie1 extracellular domain (ECD) or C-terminal tail (CT) were used. (B) qRT-PCR analysis of *Tie1* and *Tie2* mRNA fold changes in lungs at the indicated time points after LPS treatment, normalized to *Pecam1*. (C) qRT-PCR analysis of *Ang1* mRNA fold changes in lungs, normalized to *Gapdh*. n = 3-6 (except n = 2 for 12 h). ** P < 0.01, *** P < 0.001 vs. PBS control, 1-way ANOVA followed by Dunnett's post hoc test.

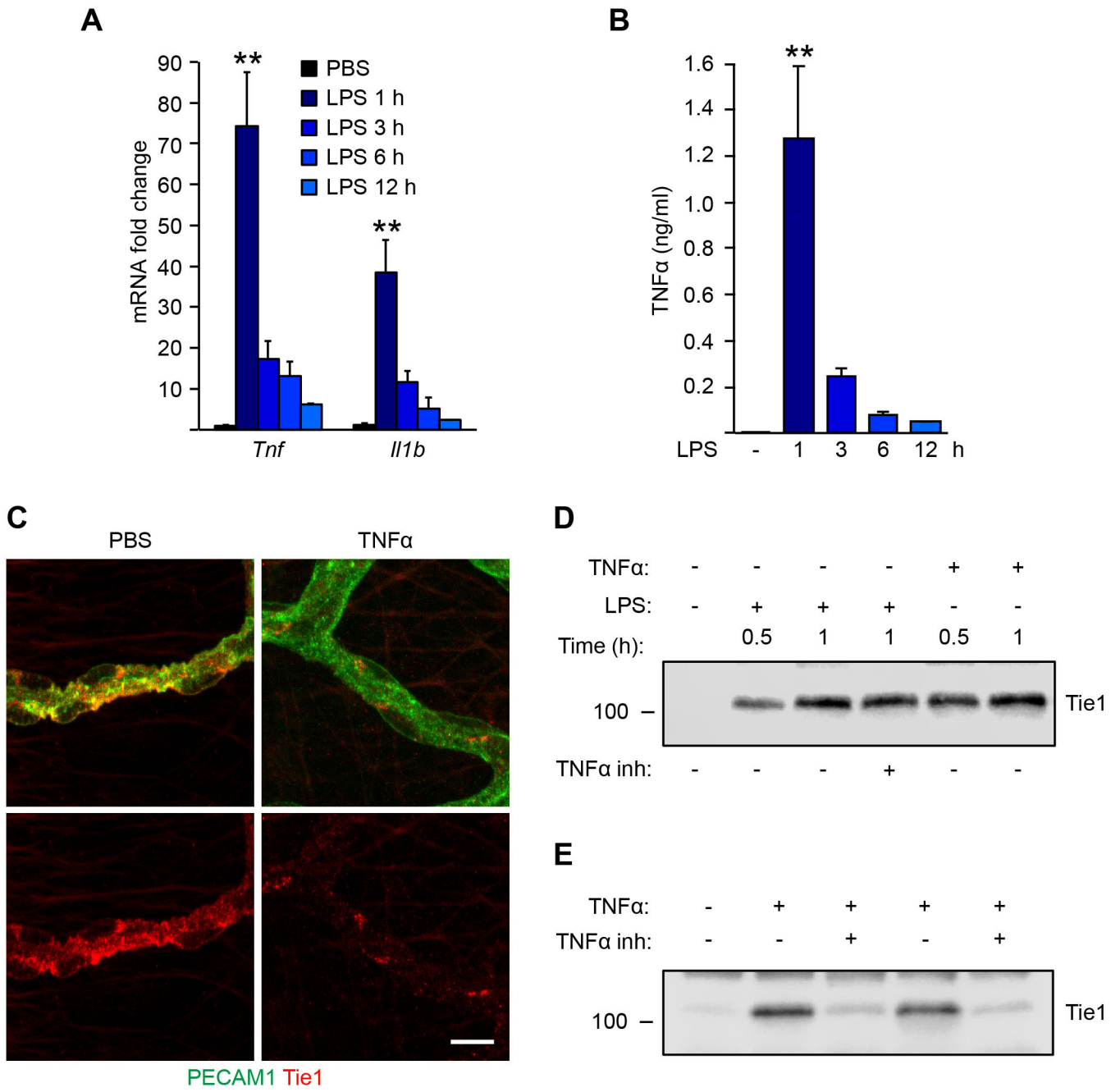

Supplemental Figure 14. TNF-α induces Tie1 cleavage in vivo. (A) qRT-PCR analysis of *Tnf* and *Il1b* mRNA fold changes in the lungs of PBS or LPS treated mice at the indicated time points, normalized to *Gapdh* mRNA expression. (B) TNF-α protein (ng/ml) in serum of LPS treated mice at the indicated time points. Error bars: SEM. ** $P < 0.05$, LPS 1 h (n = 3) vs. PBS control (n = 2), 1-way ANOVA followed by Dunnett's post hoc test. (C) Tie1 ECD (red) and PECAM1 (green) staining in tracheal blood vessels. Representative fluorescent images (n = 3). Scale bar: 10 µm. (D) Tie1 western blotting from serum of TNF-α, LPS and soluble TNF-α receptor (TNF-α inhibitor) treated mice at the indicated time points. Representative western blot (n = 3). (E) Tie1 western blotting from serum of TNFα, and TNFα +TNFα inhibitor treated mice. n = 2 (except for PBS control n = 1).

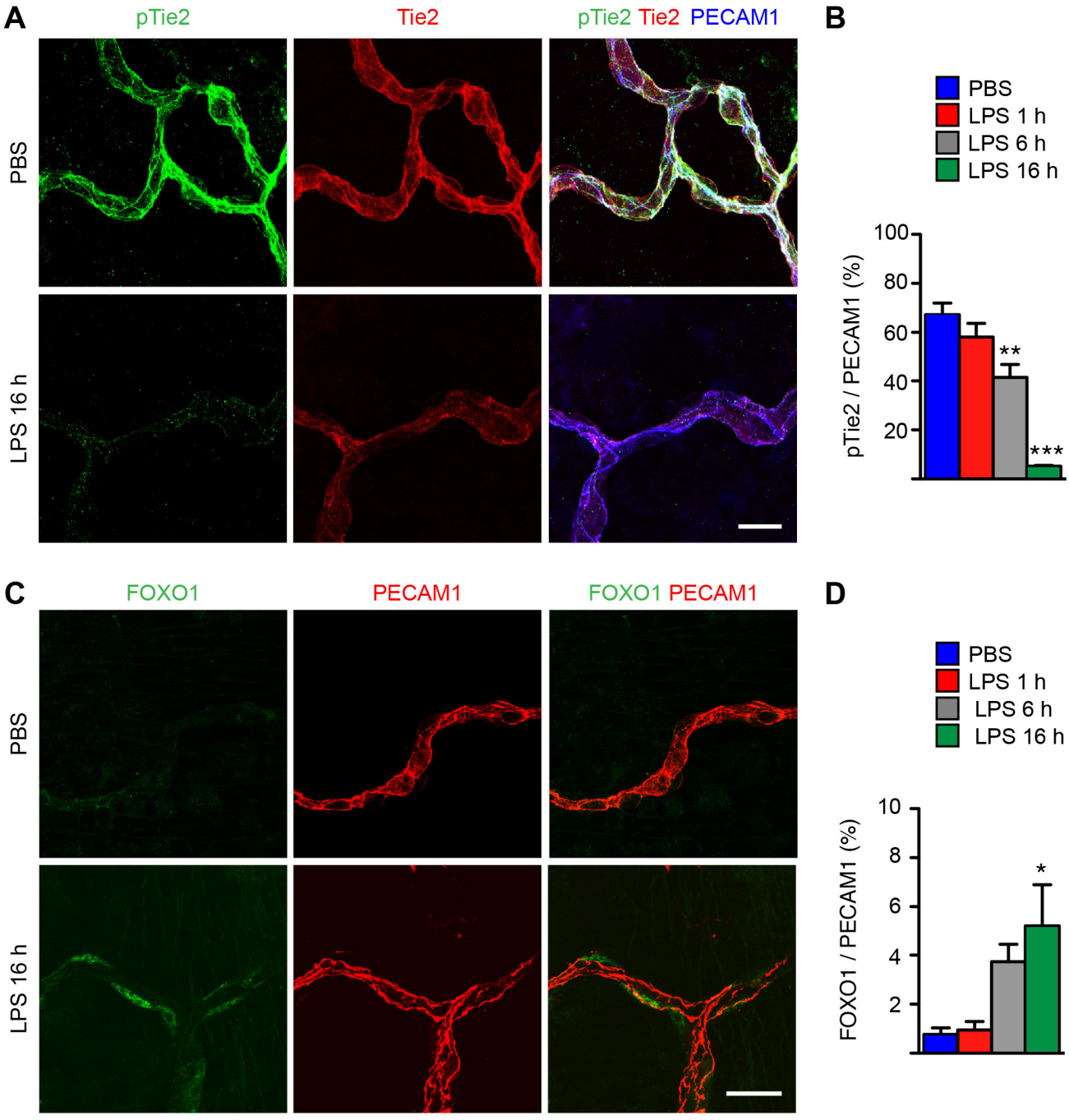

Supplemental Figure 15. Effect of LPS on Tie2 phosphorylation and FOXO1 expression. (A) Phospho-Tie2 (green), Tie2 (red) and PECAM1 (blue) staining in tracheal blood vessels of PBS or LPS treated mice. (B) Quantification of phospho-Tie2 relative to PECAM1 (%) at the indicated time points. (C) FOXO1 (green) and PECAM1 (red) staining. (D) Quantification of FOXO1 relative to PECAM1 (%). Scale bars: 20 µm. n = 3. * $P < 0.05$, ** $P < 0.01$, *** $P < 0.001$ vs. PBS control, 1-way ANOVA followed by Bonferroni's post hoc test.

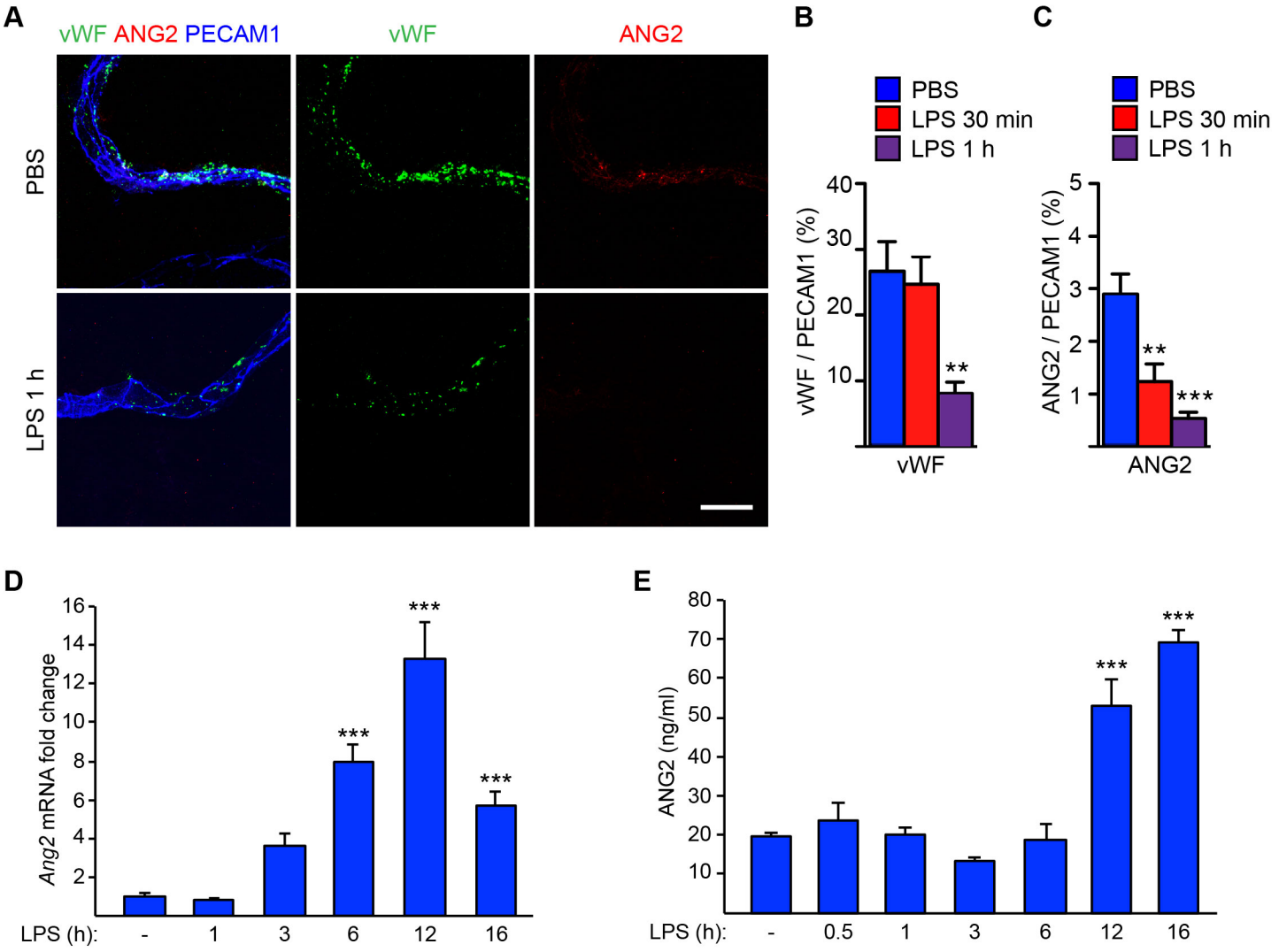

Supplemental Figure 16. Effect of LPS on ANG2 expression and release. (A) vWF (green), ANG2 (red) and PECAM1 (blue) staining in tracheal blood vessels in PBS and LPS treated mice. Scale bar: 20 µm. (B) Quantification of vWF relative to PECAM1 (%) at the indicated time points. (C) Quantification of ANG2 relative to PECAM1 (%). n = 3. ** P < 0.01, *** P < 0.001 vs. PBS control, 1-way ANOVA followed by Bonferroni's post hoc test. (D) qRT-PCR analysis of *Ang2* mRNA fold changes in the lungs of PBS or LPS treated mice at the indicated time points, normalized to *Pecam1*. n = 3-6 (except n = 2 for 12 h). (E) Concentration of ANG2 protein in serum (ng/ml). n = 3-9 (except n = 2 for 0.5 and 12 h). ** P < 0.01, *** P < 0.001 vs. PBS control, 1-way ANOVA followed by Dunnett's post hoc test.

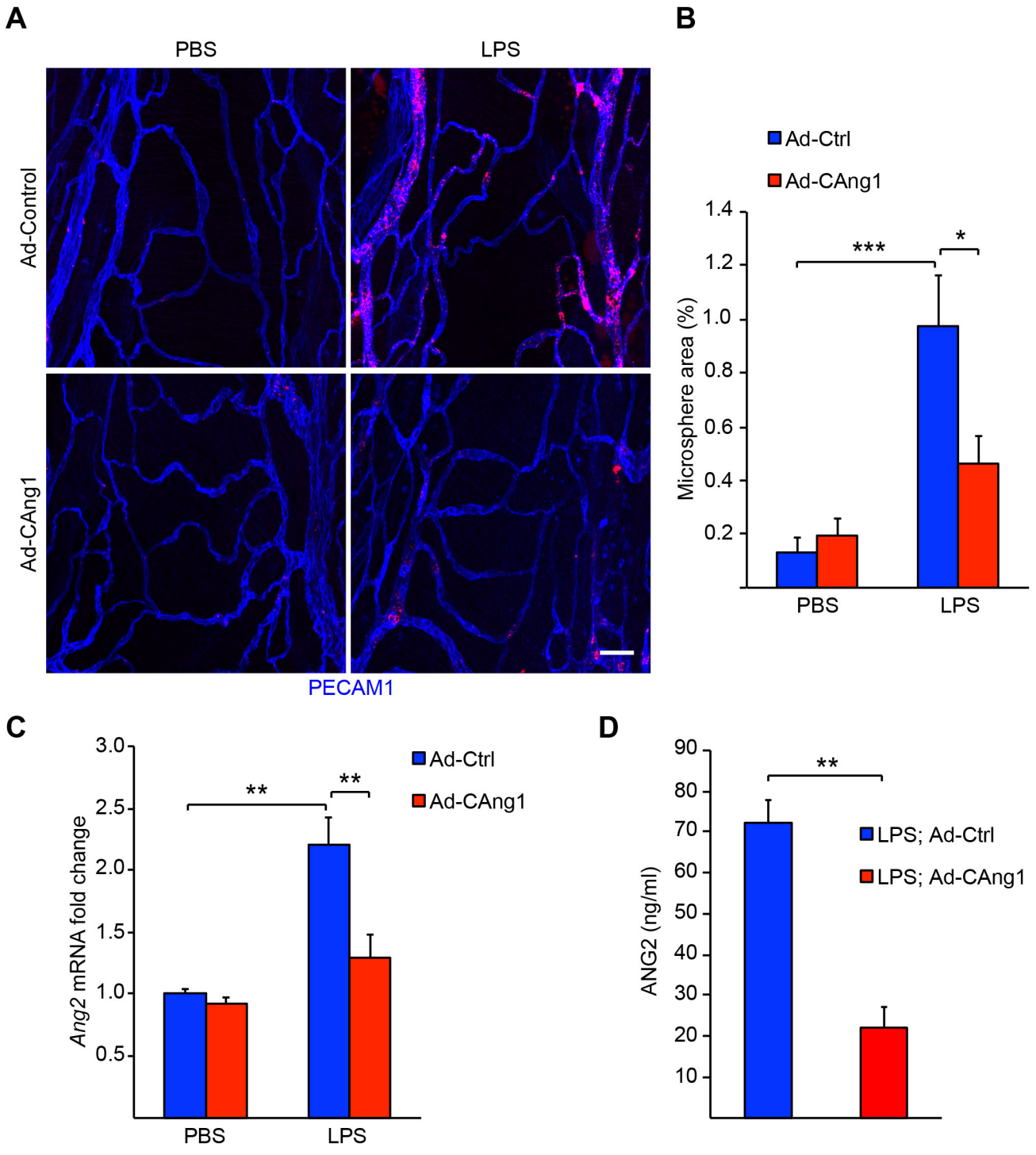

Supplemental Figure 17. ANG1 reduces LPS-induced leakage and ANG2 mRNA and protein. (A) Representative images of fluorescent microsphere leakage 16 h after LPS injection in tracheal blood vessels stained for PECAM1 (blue) in mice treated with Ad-control or Ad-CAng1. Vascular leakage was analyzed as explained in the Methods. Scale bar: 50 µm. (B) Quantification of microsphere area per field (%). (C) *Ang2* mRNA fold change in the lungs normalized to *Pecam1* and (D) ANG2 protein concentrations in serum 16 h after LPS injection. n=3-10. Error bars: SEM. Scale bar: 50 µm. * P < 0.05, ** P < 0.01, *** P < 0.001, 1-way ANOVA followed by Tukey's post hoc test (B-C) or Student's t-test (D).